DETERMINATION OF THE VELOCITY PROFILE IN AN ARGON PLASMA

Erno S. Daniel

Spalding Laboratories
California Institute of Technology

Approved:
W. H. Corcoran

TABLE OF CONTENTS

LIST OF TABLES

LIST OF GRAPHS

LIST OF FIGURES

Boron nitride powder is injected into a pure argon gas plasma. The particles which glow due to the high temperatures in the plasma are used as tracers for the velocity measurement. The motion of the particles is recorded by photographic techniques. The results obtained are compared with values calculated from the temperature field in the plasma.

INTRODUCTION

The purpose of the velocity measurements described in this paper was to obtain the velocity field within the argon plasma jet and its cooling jacket both as a function of radial and as a function of axial position. The major problem in measuring velocities in this particular plasma jet was the fact that the extremely high temperatures in the jet prohibit the use of conventional methods. Mechanical velocity probes would melt, or else disturb the flow of the gas in the plasma. The laser beam method described by Che Jen Chen[1] is also not applicable due to the extreme brightness of the radiation in this plasma, and also because of the excessive equipment it requires. Optical methods (although not very thoroughly investigated) have also been found to be inferior to the boron nitride method that was finally adopted. It was selected because of the simplicity with which it can be performed, and because it seemed to be best suited for the given circumstances of all the methods mentioned above. Boron nitride does not melt at the temperatures that are found in the plasma, but glows, which makes it easy to trace. Furthermore, the boron nitride particles do not disturb the system significantly. To double-check this method, a procedure given by C. F. Gottschlich et al.[2] for calculating the velocities theoretically from the temperature field inside the plasma was also adopted. From the temperature field values that have been found previously, velocities in the plasma were calculated by the equation

$$v = \frac{\lambda\left(\frac{\partial^2 T}{\partial r^2} + \frac{1}{r}\frac{\partial T}{\partial r} + \frac{\partial^2 T}{\partial z^2}\right) + \frac{d\lambda}{dT}\left[\left(\frac{\partial T}{\partial r}\right)^2 + \left(\frac{\partial T}{\partial z}\right)^2\right] - \varepsilon}{\rho C_p \frac{\partial T}{\partial z}}$$

and compared with the results obtained by the boron nitride method. The derivation of the equation and the assumptions made in the derivation are shown in Appendix 1.

EXPERIMENTAL INSTRUMENTATION

The plasma generator used in this experiment was a high-frequency (20Mc) induction type, capable of up to 10kw of electrical dissipation. It was obtained from the Forrest Electronic Corporation. The gas used was argon, and it was introduced in two streams (main and cooling streams) through distributor rings in order to insure a symmetric and laminar flow of the plasma. The gas flows down in a 1 3/8 inch diameter quartz tube into the atmosphere. The schematic diagram of the plasma can be seen in Figure 1. The pressure inside the plasma jet was assumed to be atmospheric. All measurements were made below the power input coil, for local thermodynamic equilibrium probably does not exist immediately near the input coil. The power supply for the high-frequency coil is water cooled. The initial electrons for igniting the jet were supplied by a carbon rod, which was touched to the inside of the tube near the power input coil. The method for injecting the boron nitride particles was arrived at after some experimentation. It was decided to inject them into the cooling stream as high axially as possible on the plasma tube, in order to disturb the jet the least. Due to the inward direction of flow of the cooling gas produced by the narrowed-down shape of the tip of the nozzle, this also assured a quite uniform distribution of boron nitride particles in the plasma. Therefore, the flow of the cooling gas was split into two, and the flow in the bypass was directed through a particle fluidizer. The fluidizer consists of a vertical glass tube with a glass frit at the lower end for holding the boron nitride particles. The argon gas enters at the bottom and passes through the frit. It leaves via a sidearm, carrying the boron nitride particles which are placed into the fluidizer through another sidearm on the opposite side. The design of the fluidizer and the flow diagram of the system can be seen in Figure 2. A photograph of the system is shown in Figure 3. A camera was employed for recording the motion of the boron nitride particles. It was a 35 mm Honeywell-Pentax H3V model camera, equipped with a Super-Takumar 100 mm telephoto lens, 1:1.8/55. TRI-X PAN film was used. The pictures were developed in the darkroom of the laboratory.

EXPERIMENTAL PROCEDURES

As indicated before, the experimental procedure consisted of two entirely separate parts. In the first part the velocities were calculated theoretically from temperature data, which have been determined previously by spectroscopic methods by Satish V. Desai[3]. These temperature field values are given in Table 1 and Graph 1. The calculations were performed by computer for 96 data points. This method had the advantage of not disturbing the flow in the plasma, and of having excellent spatial resolution. The results of the calculations are shown in Table 2 and Graph 2.

The other part of the experiment consisted of measuring the velocities with the help of boron nitride particles. These particles were kept to a size so that their diameters were between 40 and 80 microns. This insured a minimum gravitational effect on their downward motion in the plasma, and also kept them small enough not to disturb the plasma flow too much. But it also kept them large enough not to evaporate before they could be detected in the plasma. Great care was first of all taken to preserve the same flow conditions for all of the tests. The current on the power input coil was always set to the same value, and the gas flow was also always adjusted to a rate of 7 liters/sec for the mainstream, and 12 liters/sec for the cooling stream. The bypass valve was first closed, and the plasma jet was ignited and allowed to stabilize. Then the bypass valve was opened slightly, just far enough to fluidize the boron nitride particles, and the particles were thus allowed to enter the plasma stream. Their presence was immediately noticeable in the stream due to the greenish glow they impart to the jet due to their evaporation. Photographs were then taken at a shutter speed of 1/1000 of a second, and the negatives were developed. A typical photograph can be seen in Figure 4.

To obtain the exact positions of the particles in the plasma, a new sort of three dimensional photography was employed. The sideview of the plasma was reflected with the help of a mirror into the camera, so that the front and sideviews of the tube could be seen side by side on the photographic film. (See Figure 4) The sideview of the plasma jet was obtained by placing the mirror so that the angle of incidence of the rays from the side of the tube was equal to the angle of their reflection into the photographic lens. From these two views, which give the two cartesian coordinates of the particles, the exact radial position of each particle can be determined. The axial and radial positions of the particles, as well as the lengths of the streaks they left during the 1/1000 of a second exposure time on the photographic film were measured exactly on each photographic negative with the help of a measuring magnifier. These values were then converted into lengths in inches. The scale factor was determined by comparing the diameter of the plasma tube as it appeared on the negatives with its actual diameter.

In order to determine the exact velocities, next the camera shutter had to be calibrated. This was done with the help of a synchronous electric motor, whose rotational frequency was known to be exactly 3000 rpm. A disk into which slits were cut was attached to the shaft of the motor. A flash-bulb was attached behind the disk, and the motor was brought up to constant rotational frequency. Several pictures of the rotating disk were taken. An example of these pictures can be seen in Figure 5. From the lengths of the streaks that the slits left on the photographic negative, the shutter speed of the camera was exactly determined.

Using this calibration factor, the lengths of the boron nitride particle streaks were converted into velocities, and then the raw data was fit by computer by a fourth degree equation. The curves for specified axial positions were determined. The results of the measurements with boron nitride particles are shown in Table 3 and Graph 3.

RESULTS AND DISCUSSION

If the two sets of results given in Tables 2 and 3 and Graphs 2 and 3 are compared, it can be seen that the measured velocities are about 30% lower than the calculated ones. Though such a large discrepancy is quite difficult to explain, an attempt will be made to find all possible sources of error, and to suggest where such a discrepancy could originate.

The first possibility is, of course, that the temperature field inside the plasma is different under the present set of circumstances than it was when it was previously determined. This, of course, could account for all of the discrepancy very easily, and could be checked by repeating the spectroscopic temperature measurements. But let us analyze all possible sources of errors.

Let us talk further about the errors in the velocities calculated from the temperature field. First of all, the temperature values have a probable error of about ±3%. In the calculations the first and second derivatives of the temperature field are used, as well as T itself to the powers .703 and -.297. The shapes of the curves, however, are quite correct, because the error is in their position and not their shape. Therefore, the derivative values are probably accurate to within 1%. Constants that have been used in the calculations are taken from scientific journals. Their error bands are as follows:

(thermal conductivity)[4]	$<$ 10%
(heat capacity of argon)[5]	$<$ .5%
(gas constant)[6]	$<$ .1%

We can see then that the greatest source of error in the calculated results is due to the error in thermal conductivity values. This is a multiplicative factor in the calculations, and therefore, imparts an error band of about 10% to the velocities. For this reason, it is possible that they are too high by a few percent. Another factor that could make these velocity values too high is the fact that the emissivities of argon in the plasma were assumed to be negligible. Now especially in the hotter parts of the plasma, this is not necessarily true, for emissivities could amount to a few percent. Since the emissivities should be subtracted in the calculations, the results in the high temperature regions could again be high by a few percent. A third small factor in the calculations that could account for the discrepancy is the fact that laminar flow within the plasma is assumed. However, in observing the motion of the boron nitride particles, some of them were found to have small radial velocity components, amounting to 1-2%. If the plasma flow indeed has such radial components, then the calculated velocities which assume laminar flow are again 1-2% high. All of these factors then make it possible for the calculated velocities to be high by approximately 10%.

The errors in the measurements are due mainly to the fact that the plasma flow is disturbed by the injection of the boron nitride particles. Though great care was taken to obtain the same flow rates for all tests, and a circular distributor ring was used in order to insure the symmetric distribution of the gas coming in through the bypass, and the plasma was given time to stabilize, still the entry of the boron nitride particles has some effect on the flow. The greatest part of this effect is the fact that they not only glow, but also vaporize to some extent in the plasma stream. This has a slowing down effect on the particles, and could result in measured velocities that are too low. Gravitational effects, which counteract this slowing down have been considered, but were found to be only .2% for the diameter of particles that were used. Therefore, the results here could be low by a couple of percent, due mainly to the vaporization of the particles.

The greatest source of error at present is in the calibrations. Here the shutter action of the camera must be explained in some detail. The shutter actually consists of a narrow slit which moves across the photographic film with a certain velocity.

If an object photographed is also moving in the direction of the motion of the slit, it will be exposed for a longer time. The distance that any point traces out on the photographic film if moving in the same direction as the slit is $D=w(1+(v_2/v_1-v_2))$, where w is the width of the slit, v_1 the velocity of the slit, and v_2 the velocity of the moving object. Therefore the streaks left by the slits on the top half and the bottom half of the rotating disk will be of unequal length. Now in the calibrations it was assumed (since the streak lengths covered most of a circular path) that the total integrated velocity component of each moving point on the slits on the upper half of the picture would be equal to that on the lower half of the picture, and therefore would cancel out if the two were averaged. But due to the fact that there are five slits on the disk, this is not exactly true, and has led to a probable error of approximately ±6%. If the calibration value were lower, the velocity values would be again higher, reducing the discrepancy.

CONCLUSIONS AND RECOMMENDATIONS

It is safe to assume that the actual velocities lie somewhere between the calculated and the measured velocities. Actually, both sets of results are correct, and the difference between them is due to the fact that the temperature fields are different. The precision, however, is approximately 10% by either method.

Several things could be done to obtain more agreeable results. First, new temperature readings could be taken under the present circumstances, and probably much closer agreement could be reached between the calculated and measured results. The calibration of the camera could also be improved by using a disk with point slits which are distributed symmetrically in the disk. This would increase the precision. By these methods, even though the rms error in the measured velocities could not be brought under 5%, the accuracy could be greatly increased.

However, these methods prove to be very good, for the calculation method allows velocities to be determined simultaneously with temperature determinations, and the boron nitride method can be used any other time when the plasma is in operation.

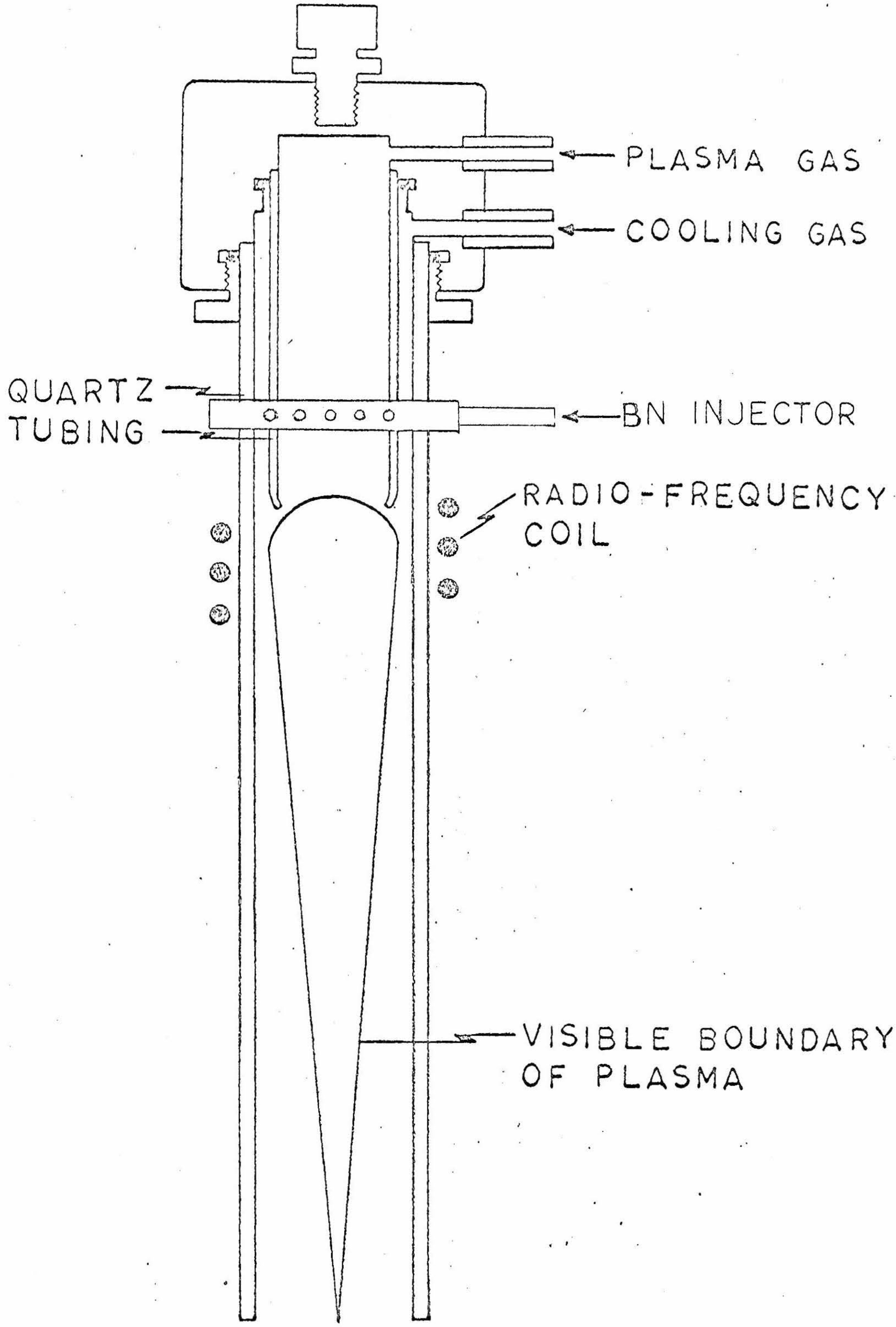

FIG. 1. PLASMA REACTOR ASSEMBLY

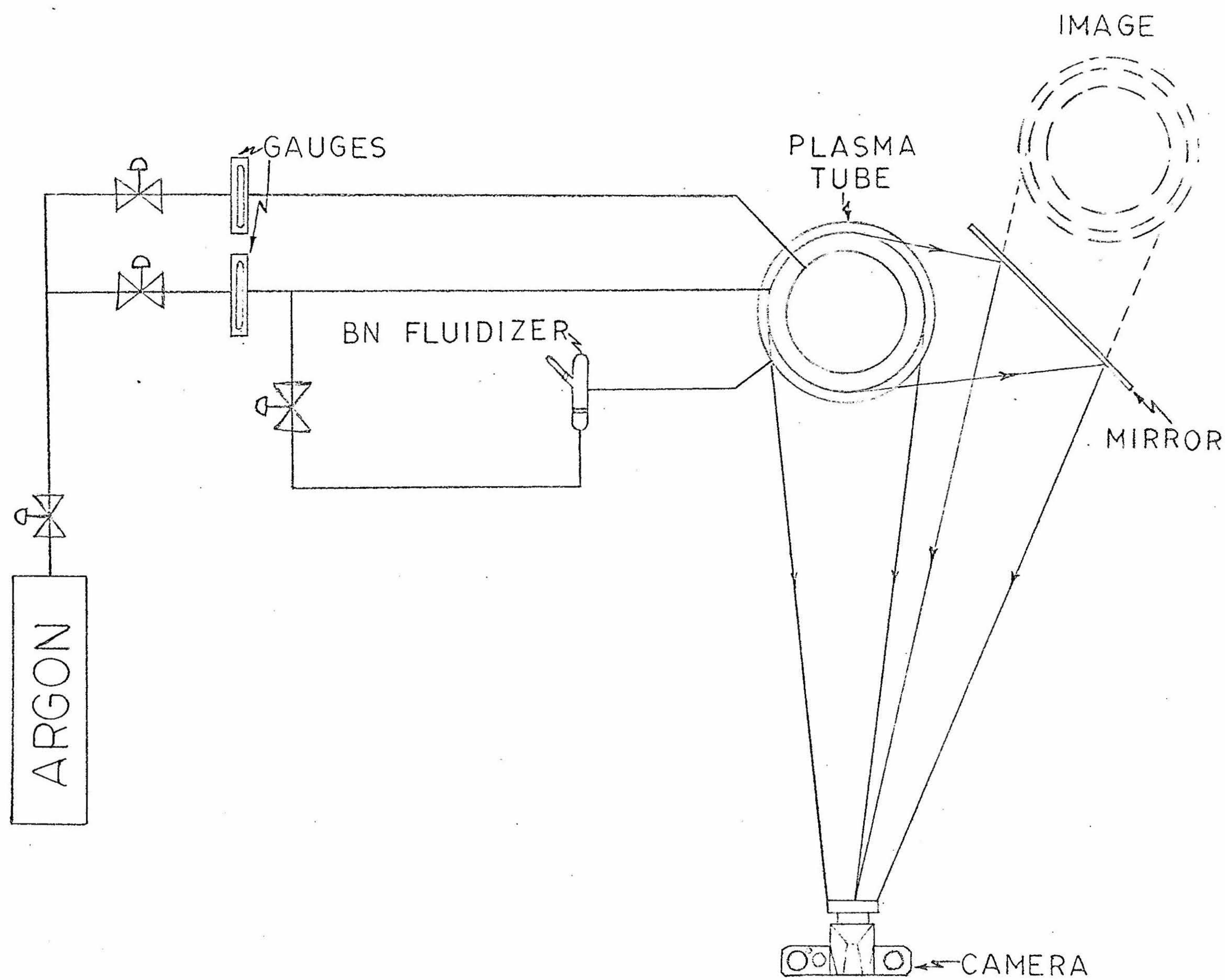

FIG. 2. EXPERIMENTAL SETUP

FLUIDIZER PLASMA JET

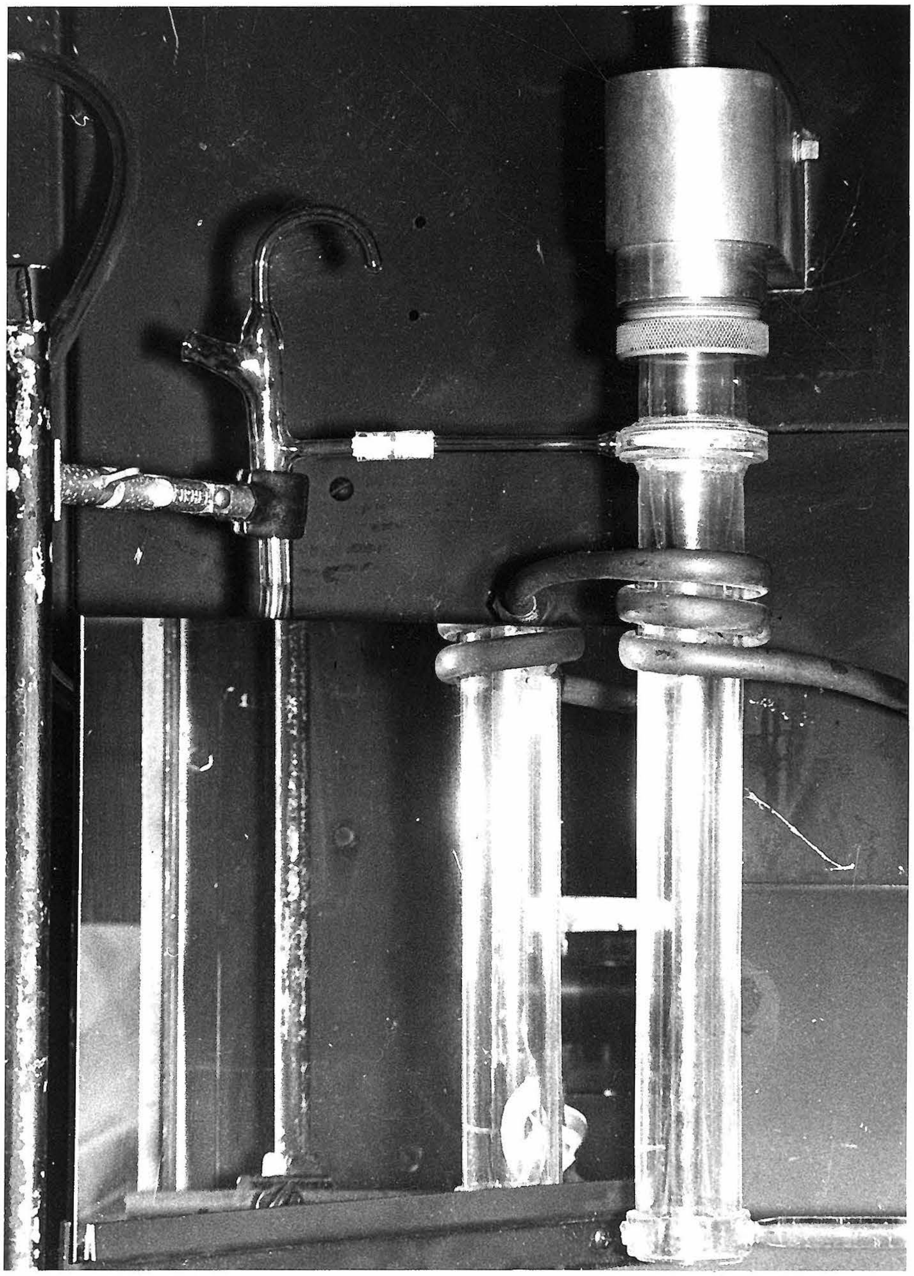

MIRROR IMAGE

FIG. 3. PHOTOGRAPH OF EXPERIMENTAL SETUP

FRONT VIEW

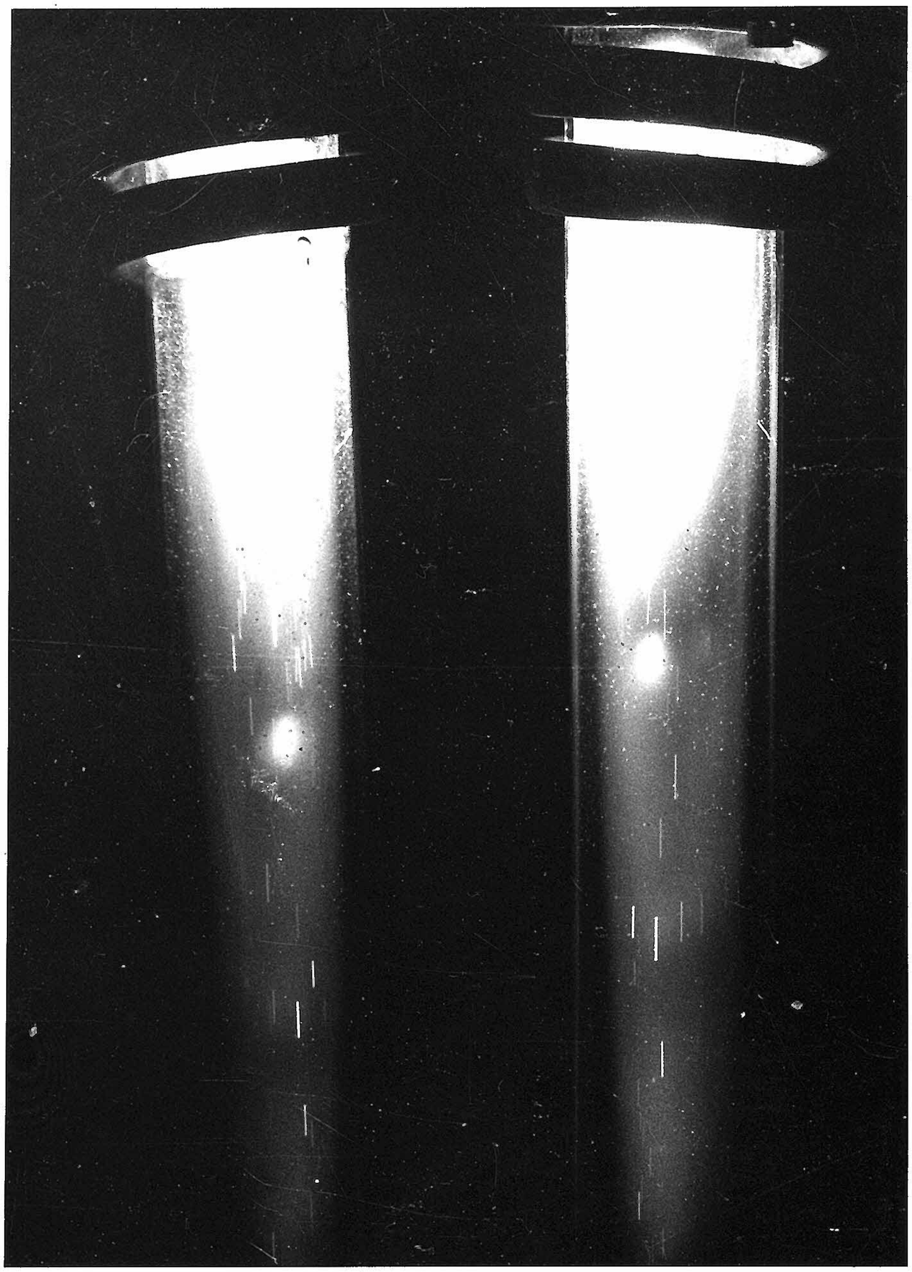

REFLECTED SIDE VIEW

FIG. 4. SAMPLE PICTURE FOR VELOCITY DETERMINATION

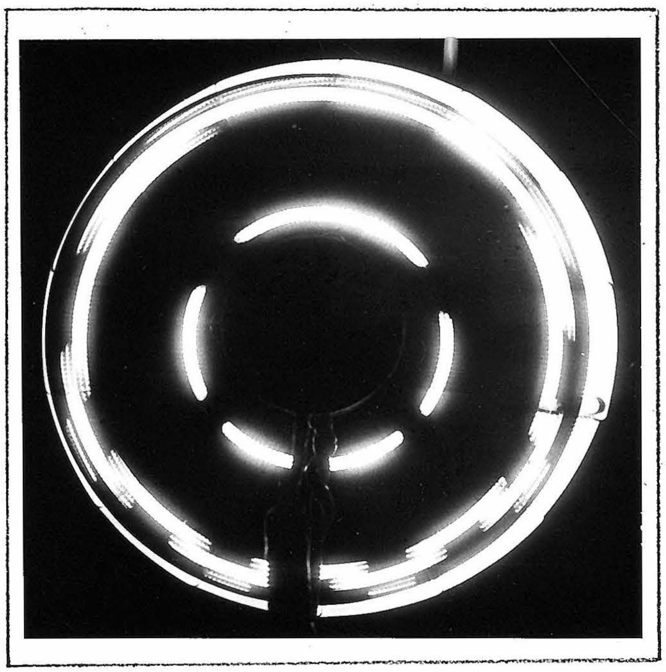

FIG. 5 SAMPLE CALIBRATION PICTURE.

TABLE 1

TEMPERATURE FIELD VALUES

Axial pos.	1.64	1.84	2.24	2.64	3.04	3.44
Radial pos.						
.00	6020	5900	5781	5660	5540	5420
.025	6014	5898	5779	5655	5532	5406
.05	6010	5895	5776	5652	5532	5407
.075	6006	5890	5770	5647	5531	5410
.10	6001	5882	5761	5640	5526	5407
.125	5992	5870	5749	5628	5514	5394
.15	5978	5854	5734	5612	5494	5370
.175	5960	5835	5715	5591	5466	5334
.20	5937	5811	5693	5564	5431	5288
.225	5908	5783	5667	5533	5388	5233
.25	5873	5751	5636	5494	5338	5170
.275	5833	5714	5599	5448	5280	5099
.30	5786	5671	5554	5391	5211	5017
.325	5733	5623	5500	5320	5127	4920
.35	5674	5566	5431	5230	5019	4797
.375	5606	5499	5345	5114	4879	4636

Axial and radial positions are given in inches, temperatures in ^{o}K.

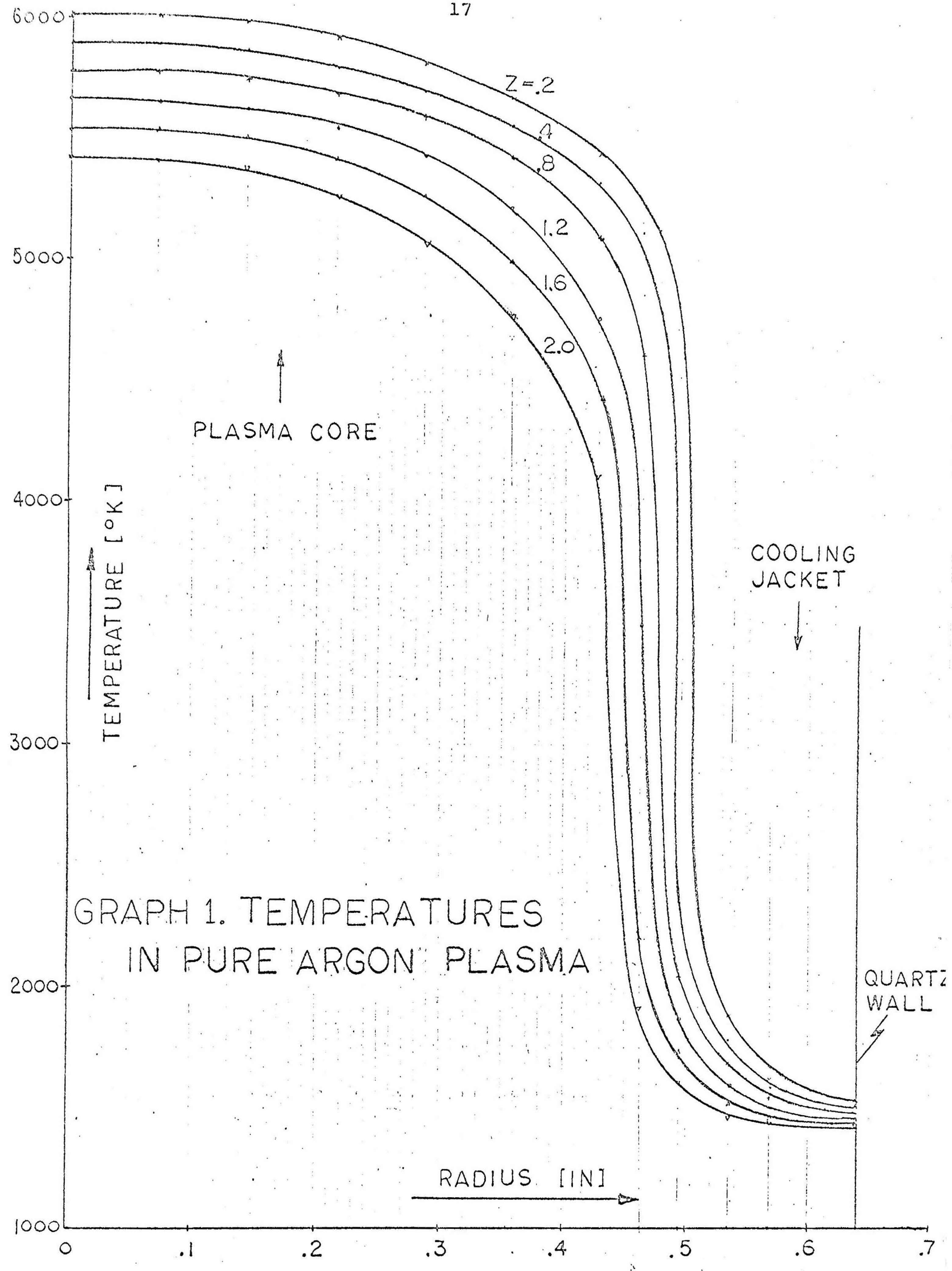
6000
5000
4000
3000
2000
1000
Z=.2
.4
.8
1.2
1.6
2.0
PLASMA CORE
TEMPERATURE [°K]
COOLING
JACKET
QUARTZ
WALL
GRAPH 1. TEMPERATURES
IN PURE ARGON PLASMA
RADIUS [IN]
0
.1
.2
.3
.4
.5
.6
.7

TABLE 2

CALCULATED VELOCITIES

Axial pos.	1.64	1.84	2.24	2.64	3.04	3.44
Radial pos.						
.00	538.8	519.8	501.2	482.7	464.5	446.8
.025	537.8	519.4	501.0	482.0	463.4	444.8
.05	537.2	518.9	500.5	481.5	463.3	444.8
.075	536.6	518.1	499.6	480.8	463.2	445.3
.10	535.7	516.9	498.2	479.6	462.5	444.8
.125	534.2	515.1	496.4	477.8	460.7	443.0
.15	532.1	512.6	494.0	475.4	457.7	439.4
.175	529.2	509.5	491.1	472.2	453.6	434.1
.20	525.5	505.8	487.7	468.3	448.3	427.4
.225	521.0	501.5	483.7	463.5	442.1	419.5
.25	515.5	496.5	479.0	457.8	434.8	410.5
.275	509.2	490.9	473.5	450.9	426.4	400.5
.30	502.0	484.4	466.7	442.5	416.4	389.1
.325	493.9	477.0	458.5	432.2	404.4	375.6
.35	484.8	468.5	448.4	419.1	389.3	358.9
.375	474.6	458.5	435.8	402.6	370.0	337.5

Axial and radial positions are given in inches, velocities in inches/sec.

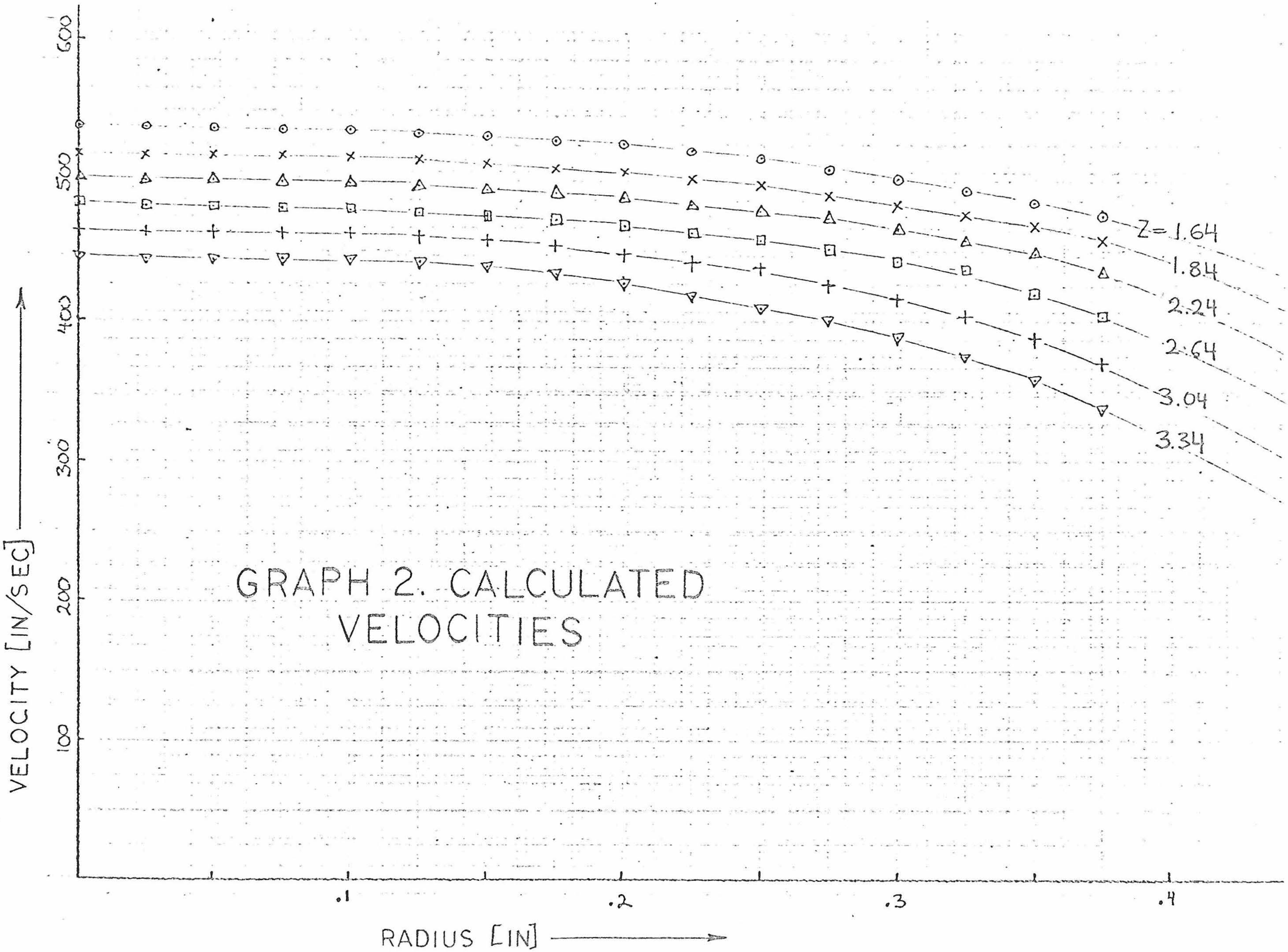

GRAPH 2. CALCULATED VELOCITIES

TABLE 3

MEASURED VELOCITIES

Axial pos.	1.64	1.84	2.24	2.64	3.04	3.44	4.00	4.50
Radial pos.								
.00	354	344	326	310	297	287	278	274
.025	354	344	326	311	298	287	276	270
.05	353	344	326	311	297	286	274	267
.075	351	342	325	310	296	285	271	263
.1	348	339	323	308	294	282	268	258
.125	345	336	319	304	291	279	264	253
.15	340	331	315	300	287	275	260	248
.175	334	326	310	296	282	270	255	243
.2	327	319	304	290	277	264	249	237
.225	319	311	296	283	270	258	243	232
.25	310	302	288	275	263	251	237	225
.275	300	293	279	266	254	243	229	219
.3	289	282	269	256	245	235	222	212
.325	277	270	257	246	235	225	214	205
.35	264	257	245	234	224	215	205	197
.375	250	244	232	221	212	204	195	190
.4	235	229	218	208	200	193	186	181
.425	219	213	202	193	186	180	175	173
.45	202	196	186	178	172	167	164	164
.475	183	178	169	161	156	153	153	155
.5	164	159	150	144	140	139	140	146
.525	144	139	131	126	123	123	128	137

Axial and radial positions are given in inches, velocities in inches/sec.

These points are from the hand-smoothed curves drawn through the data points.

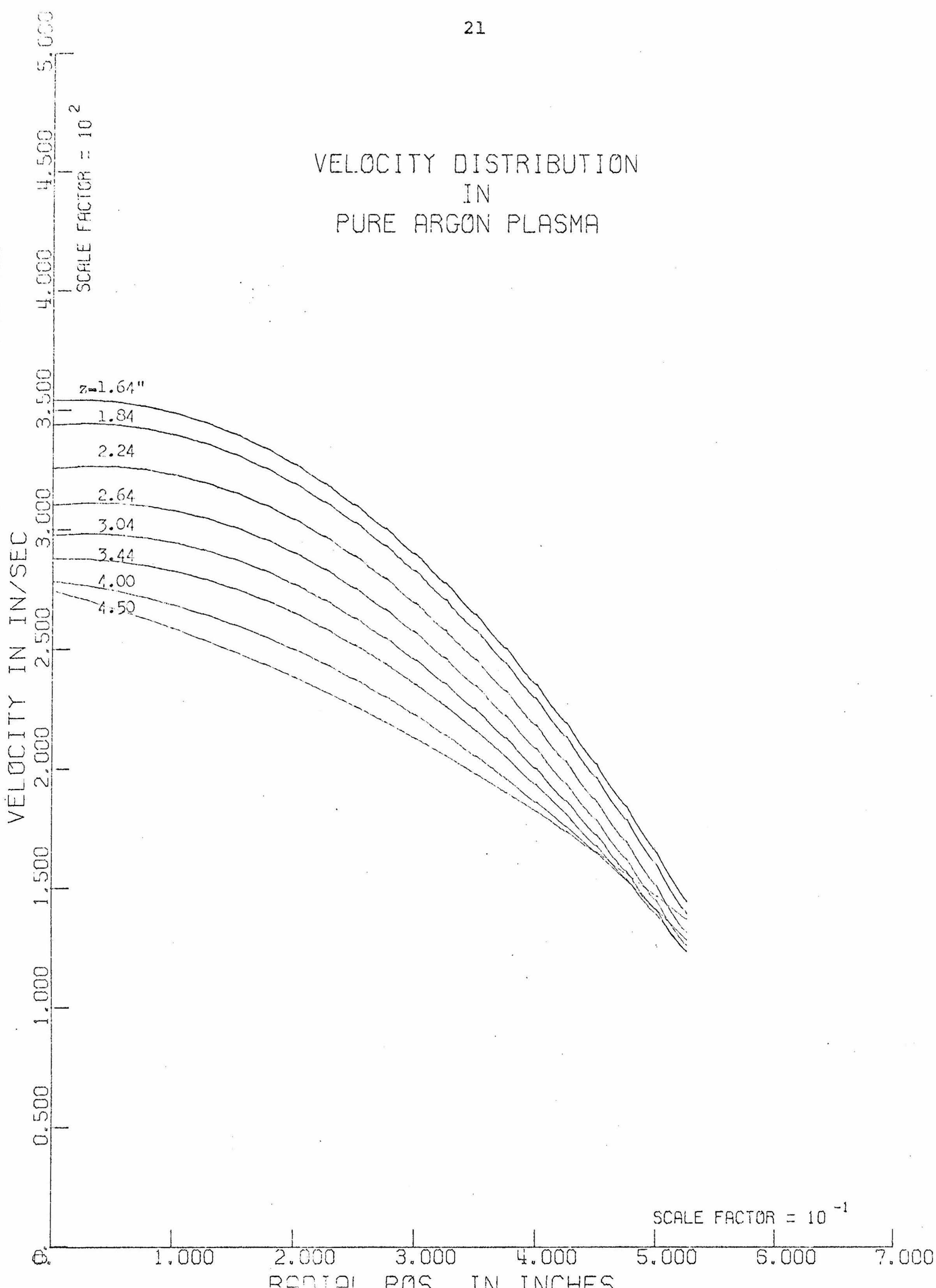
VELOCITY DISTRIBUTION
IN
PURE ARGON PLASMA
z=1.64"
1.84
2.24
2.64
3.04
3.44
4.00
4.50
VELOCITY IN IN/SEC
SCALE FACTOR = 10 2
SCALE FACTOR = 10 -1
0.
0.500
1.000
1.500
2.000
2.500
3.000
3.500
4.000
4.500
5.000
1.000
2.000
3.000
4.000
5.000
6.000
7.000

APPENDIX

DERIVATION OF THE EQUATION RELATING THE TEMPERATURES AND VELOCITIES IN AN ARGON PLASMA

The total energy balance equation gives

$$\frac{\partial}{\partial t}\rho(U+\tfrac{1}{2}v^2) = -\nabla\cdot\rho\underline{v}(U+\tfrac{1}{2}v^2) - \nabla\cdot q - \varepsilon + \rho\underline{v}\cdot g - \nabla\cdot p\underline{v} - \nabla\cdot\underline{\underline{\tau}}\cdot\underline{v} \quad (1)$$

The mechanical energy balance equation gives

$$\rho\frac{\partial}{\partial t}(\tfrac{1}{2}v^2) = -\rho\underline{v}\cdot\nabla(\tfrac{1}{2}v^2) + p\nabla\cdot\underline{v} + \rho(\underline{v}\cdot\underline{g}) - \nabla\cdot\underline{\underline{\tau}}\cdot\underline{v} + \underline{\underline{\tau}}:\nabla\underline{v} \quad (2)$$

(Total energy - mechanical energy) = Non-mechanical energy

$$\rho\frac{\partial U}{\partial t} + \rho U\cdot\nabla U = -(\nabla\cdot\underline{q}+\varepsilon) - p\nabla\cdot\underline{v} - \underline{\underline{\tau}}:\nabla\underline{v}$$

which reduces to

$$\rho\frac{DU}{Dt} = -(\nabla\cdot\underline{q}+\varepsilon) - p\nabla\cdot\underline{v} - \underline{\underline{\tau}}:\nabla\underline{v} \quad (3)$$

The first law of Thermodynamics gives

$$dU = C_p\,dT - p\,dV - T\left(\frac{\partial V}{\partial T}\right)_p dp \quad (4)$$

which implies

$$\rho\frac{DU}{Dt} = \rho C_p\frac{DT}{Dt} - \left(\frac{\partial \ln V}{\partial \ln T}\right)_p\frac{Dp}{Dt} + \frac{p}{\rho}\frac{D\rho}{Dt} \quad (5)$$

The continuity equation says that

$$\frac{D\rho}{Dt} = -\rho\nabla\cdot\underline{v}$$

which reduces equation (5) to

$$\rho C_p\frac{DT}{Dt} = -(\nabla\cdot\underline{q}+\varepsilon) - \frac{Dp}{Dt}\left(\frac{\partial \ln V}{\partial \ln T}\right)_p - \underline{\underline{\tau}}:\nabla\underline{v}$$

or written in terms of fixed coordinates (ordinary partial derivatives)

$$\frac{\partial}{\partial t}(\rho C_p T) = -\nabla\cdot\rho C_p T \underline{v} - (\nabla\cdot\underline{q} + \varepsilon) - \underline{\underline{\tau}} : \nabla\underline{v} + \left(\frac{\partial \ln V}{\partial \ln T}\right)_p \left(\frac{\partial p}{\partial t} + \underline{v}\cdot\nabla p\right) + \rho T\left(\frac{\partial C_p}{\partial t} + v\cdot\nabla C_p\right) \tag{6}$$

Now let us make the following assumptions:

1. Steady state $\left(\frac{\partial}{\partial t} = 0 \right)$
2. Isobaric conditions $\left(\frac{\partial p}{\partial} = 0 \right)$
3. Viscous dissipation negligible $\left(\underline{\underline{\tau}} : \nabla\underline{v} = 0 \right)$
4. Ideal gas behavior $\left(\rho = \frac{p}{RT} \right)$

Then equation (6) reduces to

$$-\nabla\cdot\rho C_p T v - (\nabla\cdot\underline{q} + \varepsilon) + \rho T \underline{v}\cdot\nabla C_p = 0 \tag{7}$$

Together with the continuity equation, and with this gives

$$\rho \underline{v} C_p \left(\frac{\partial T}{\partial z}\right) = \nabla\cdot\lambda\nabla T - \varepsilon \tag{8}$$

Solving this for v, we obtain the desired equation

$$v = \frac{\lambda\left(\frac{\partial^2 T}{\partial r^2} + \frac{1}{r}\frac{\partial T}{\partial r} + \frac{\partial^2 T}{\partial z^2}\right) + \frac{\partial \lambda}{\partial T}\left[\left(\frac{\partial T}{\partial r}\right)^2 + \left(\frac{\partial T}{\partial z}\right)^2\right] - \varepsilon}{\rho C_p \frac{\partial T}{\partial z}}$$

The symbols used in the above derivation are the following:

$\frac{\partial}{\partial t}$ .... ordinary partial derivative with respect to time

$\frac{D}{Dt}$ .... subst. derivative with respect to moving frame of reference

U .... internal energy/unit mass

$\underline{v}$ .... velocity (cm/sec)

$\underline{q}$ .... heat flux (cal/sec-cm2)

ρ .... mass density (g-moles/cm^3)

$\underline{\underline{\tau}}$ .... sheer stress (dynes/cm^3)

$\underline{g}$ .... body forces (dynes/cm^3)

$\mathcal{E}$ .... total energy radiation function, or emissivity (cal/sec-cm^3)

p .... pressure (atm)

R .... gas constant (cm^3-atm/g-mole-°K)

C_p .... specific heat (cal/°K-g-mole)

V .... specific volume (cm^3/g-mole)

T .... absolute temperature (°K)

λ .... thermal conductivity (cal/cm-sec-°K)

∇ .... gradient operator

REFERENCES

[1] Che Jen Chen, "Velocity-Profile Measurement in Plasma Flows Using Tracers Produced by a Laser Beam," J. Appl. Phys., 37,8, (July, 1966)

[2] C. F. Gottschlich, J. A. Engright, and F. C. Cadek, "Measurement of the Velocity Distribution in a Plasmajet," AIAA Technical Notes, 4, 6, (June, 1966) p. 1085.

[3] H. J. Astheimer and S. V. Desai, "The Transport of Mass and Energy in an Argon Plasma Reactor," (unpublished), Chemical Engineering Laboratory, California Institute of Technology, (June 19, 1967)

[4] D. J. Collins, and W. A. Menard, "Measurement of the Thermal Conductivity of Noble Gases in the Temperature Range 1500 to 5000 Degrees Kelvin," J. of Heat Transfer, ASME, (February, 1966), p. 52.

[5] NASA Sp. 3001

[6] J. H. Perry, Chemical Engineers' Handbook, McGraw-Hill Book Company, Inc., New York, 1963.